

International Journal of Pharmacology

ISSN 1811-7775





ISSN 1811-7775 DOI: 10.3923/ijp.2021.549.561



Research Article Silver/Chitosan/Ascorbic Acid Nanocomposites Attenuates Bacterial Sepsis in Cecal Ligation and Puncture Rat Model

¹Ayman Saber Mohamed, ²Saleh Al-Quraishy, ²Rewaida Abdel-Gaber and ¹Sohair Ramadan Fahmy

Abstract

Background and Objective: Sepsis is a universal that represents a physiologic, pathologic and biochemical abnormalities disorder stimulated by infection. The present study aimed to synthesize and apply silver/chitosan/ascorbic acid Nanocomposites (Ag-CS-AA NC) on septic rats induced by cecal ligation and puncture. **Materials and Methods:** The synthesized Ag-CS-AA NC were characterized by UV-visible spectroscopy, XRD, XPS, FTIR and TEM. H₂O₂ scavenging and antibacterial activities of Ag-CS-AA NC were analyzed. Eighteen rats were randomly divided into three groups: Sham group, CLP-induced sepsis and septic rats treated with Ag-CS-AA NC. **Results:** The synthesized Ag-CS-AA NC showed in vitro potent antioxidant and antibacterial activities against Gram-positive and Gram-negative bacteria. Ag-CS-AA NC administration to septic rats showed a reduction in alanine aminotransferases, aspartate aminotransferase, alkaline phosphatase, gamma-glutamyltransferase and concentrations of total proteins, albumin, creatinine, urea, uric acid, nitric oxide, while glutathione reduced and catalase increased. The histopathological investigation showed clear improvement in the hepatic and kidney architecture. **Conclusion:** The data provide the first experimental demonstration that green synthesize Ag-CS-AA NC has a therapeutic effect against sepsis-induced liver and kidney damage through its antibacterial and antioxidant activities.

Key words: Silver nanoparticles, chitosan, ascorbic acid, sepsis, cecal ligation, antibacterial, apoptosis

Citation: Mohamed, A.S., S. Al-Quraishy, R. Abdel-Gaber and S.R. Fahmy, 2021. Silver/chitosan/ascorbic acid nanocomposites attenuates bacterial sepsis in cecal ligation and puncture rat model. Int. J. Pharmacol., 17: 549-561.

Corresponding Author: Ayman Saber Mohamed, Department of Zoology, Faculty of Science, Cairo University, Giza, Egypt

Copyright: © 2021 Ayman Saber Mohamed *et al.* This is an open access article distributed under the terms of the creative commons attribution License, which permits unrestricted use, distribution and reproduction in any medium, provided the original author and source are credited.

Competing Interest: The authors have declared that no competing interest exists.

Data Availability: All relevant data are within the paper and its supporting information files.

¹Department of Zoology, Faculty of Science, Cairo University, Giza, Egypt

²Department of Zoology, College of Science, King Saud University, P.O. Box 145111, Riyadh, Saudi Arabia

INTRODUCTION

Sepsis is one of the biggest global health problems that can quickly develop severe complications for a patient if it is not dealt with early1. Sepsis is defined as the systemic response resulting from acute infection, especially for Grampositive or Gram-negative bacteria which represents a physiologic, pathologic and biochemical abnormalities disorder stimulated by infection². Staphylococcus aureus, Streptococcus pyogenes, Klebsiella spp., Escherichia coli and Pseudomonas aeruginosa are among the most commonly isolated bacteria in sepsis³. While Candida species are responsible for about 17% of sepsis, with Aspergillus and other fungi accounting for the remaining 2-3%4. The number of sepsis cases annually is estimated to exceed 30 million and lead to the death of about 6 million people⁵. Sepsis causes immune effector cells to die through apoptosis, suppresses the expression of MHC class II molecules, increases the expression of negative costimulatory molecules, increases anti-inflammatory cytokines and increases the number of regulatory T cells and myeloid-derived suppressor cells⁶. The leading causes of organ injury in sepsis tend to be inflammatory cascades and the release of cytokines, especially Tumour Necrosis Factor (TNF), Interleukin 6 (IL-6) and free radical Nitric Oxide (NO)⁷.

The capacity of the substance to restrain or eliminate cells of bacteria is called antibacterial activity⁸. Worldwide, antibiotics have been used to treat many bacterial diseases but recently, there has been considerable interest in antimicrobial resistance problems⁹. Therefore, alternatives to conventional antibiotics are urgent.

The development of nanotechnology in various fields represents a potential tool in treating different diseases ¹⁰⁻¹³. Nanoparticles consider now a viable alternative to antibiotics and seem to have a high potential to solve the emergence of bacterial Multidrug Resistance (MDR)¹⁴. Silver is a chemical element with antibacterial activity and its trends in clinical use are rising ¹⁵. One of the most well-known nanoparticles as antibacterial are silver nanoparticles (AgNPs)¹⁶. Moreover, AgNPs have proven their antibacterial ability against the MDR bacteria such as *Pseudomonas aeruginosa*, Erythromycinresistant *Streptococcus pyogenes* and ampicillin-resistant *Escherichia coli* ¹⁴. AgNPscan interact physically with the bacterial cell wall, which leads to their penetration and thus destroying the bacteria ¹⁷.

The synthesis of silver nanoparticles using an environmentally friendly method is vital in nanotechnology¹⁸. Green silver nanoparticle syntheses have recently gotten much attention because they are clean, eco-friendly, cost-

effective and easy to scale up¹⁹⁻²². Nanocomposites are high-performance composites in which at least one of the phases shows dimensions in the nanometer range (1 nm = 10⁻⁹ m)²³. Incorporating a small concentration of nanoparticles into a Nanocomposite is expected to provide maximum antibacterial properties and minimal toxicity. The synthesis of AgNPs from chitosan sources as both reducing and stabilizing agents has been paid great attention because it is considered a non-toxic, biodegradable, biocompatible and environmental-friendly material with many superior properties²⁴. Besides, chitosan exhibitions antimicrobial activity against both Gram-positive and Gram-negative bacterial strains²⁵. Because of their antimicrobial activity, Silver/Chitosan Nanocomposites are effective ingredients for wound healing and coating for medical devices²⁶.

Through a previous study²⁷, the high efficacy of silver/chitosan/ascorbic acid Nanocomposites (Ag-CS-AA NC) against microbes was proved with no cytotoxicity for human cells *in vitro*. Thereby, the present study aimed to synthesize and apply Ag-CS-AA NCon septic rats induced by Cecal Ligation and Puncture (CLP).

MATERIAL AND METHODS

Study area: The study was carried out at Department of Zoology, Faculty of Science, Cairo University, Egypt from May, 2019-March, 2020.

Chemicals: Chitosan with medium molecular weight (1278 \pm 10) and varying deacetylation degrees (>80) were purchased from India Sea Foods, Kochi, India. Acetic acid (\geq 99%), silver nitrate (AgNO₃ \geq 99%), ascorbic acid (\geq 99%) and sodium hydroxide (\geq 99%) were supplied by Sigma-Aldrich. Biochemical Kits were purchased from Bio-diagnostic Company (Dokki, Giza, Egypt).

Synthesis of silver/chitosan/ascorbic acid Nanocomposites (Ag-CS-AA NC): Ag-CS-AA NC was synthesized according to the method of Rigel-Futyra²⁷. One gram of chitosan was added to 100 mL acetic acid and heated up to 95 °C using an oil bath. Then, 7 mM AgNO₃ and 1 mM ascorbic acid solutions were added drop-wise in volume ratio (chitosan:AgNO₃: ascorbic acid, 100:20:20). The prepared mixture was kept under heating and stirring for 12-15 hrs. The mixture was dried in an electric oven (Pol-Eko) at 60 °C until complete solvent evaporation. A mixture was neutralized with 1% NaOH solution and washed with deionized water in a final step. The neutralized mixture was dried and kept in the dark until further use.

Characterization of Ag-CS-AA NC

UV-Visible spectral analysis: The synthesis of AgNPs was confirmed by UV-Vis absorption spectra. The reduction of the Ag+ions in the solution was observed by periodic sampling of the reaction mixture. A UV-Vis spectrophotometer (Shimadzu UV-1601) was used to scan the maximum absorption in the wavelength range 200-700 nm at a 10 nm interval.

X-Ray Diffraction (XRD) analysis: A Bruker D2 diffractometer analyzed the XRD patterns at 40 kV and 50 mA. The secondary graphite monochromated Co K alpha radiation ($I = 1.7902A^{\circ}$) was used and the measurements were recorded at a high angle (20) in a range of 5°-90° with a scan speed of 0.01°.

Transmission Electron Microscopy (TEM) analysis: The TEM technique was used to detect the morphology and the size of the synthesized AgNPs. A JEOL JEM-2100 transmission electron microscope operating at 200 kV was used. TEM grids were prepared by placing a drop of the particle solution on a carbon-coated copper grid and drying it under a lamp.

FTIR analysis: The material was crushed with KBr pellets for FTIR analysis and examined using a Shimadzu (model 8400) spectrum analyzer. A disk of 50 mg of KBr was prepared with a mixture of 2% finely dried sample and then examined under IR-Spectrometer. The infrared spectrum was recorded in the region of 500-4500 cm⁻¹.

X-ray Photoelectron Spectroscopy (XPS): The chemical states of the functional groups were determined using XPS. The Alpha 110 instrument from Thermo Fisher Scientific (East Grinstead, UK) was used to collect XPS data with monochromatic Al-k α (hu = 1486.7 eV) radiation and a pass energy of 20 eV. Due to ambient pollution, the binding energy of the spectra was calibrated with the C 1s peak of carbon at 284.8 eV.

Determination of silver concentration in Ag-CS-AA: Silver concentrations were measured by the Atomic Absorption Spectrophotometer (AAS) (VARIAN, Australia, model AA240 FS). The wavelength to measure absorbance was 328.1 nm. For the dissolution of nanosilver, equal volumes of the suspension and HNO $_3$ (69%) were used. Then, the solution was diluted by Milli-Q water until the Ag concentration became within the linear measuring range of the atomic absorption spectrophotometer. Analysis were performed in triplicates and the instrument detection limit for silver was 36 μg L $^{-1}$.

Antibacterial activity: The agar disc diffusion method was employed for the determination of the antibacterial activity of the Ag-CS-AA NC²⁸. Agar medium (Mueller-Hinton) was prepared by adding beef infusion solids (0.2 g), starch (15 g), casein hydrolysate (1.75 g) and agar (1.7 g) in 100 mL distilled water. Then the agar medium was sterilized by autoclaving (15 psi pressure and 120°C) for 30 min. The medium was transferred into sterilized Petri dishes in laminar airflow. After solidification of the media, overnight culture of 100 µL Escherichia coli O: 157 (ATCC 93111), Escherichia coli (ATCC 35218), Staphylococcus aureus (ATCC 25923), methicillinresistant Staphylococcus aureus (MRSA)(ATCC 43300) and Salmonella typhimurium (ATCC 14028), Clostridium perfringens and veillonella were spread separately on the solid surface of the media. Anaerobic bacteria were cultured on Schaedler anaerobic blood agar (bioMérieux, Marcy-l'Étoile, France), vancomycin-kanamycin laked blood agar and egg yolk agar for 48 hrs, at 37°C in an anaerobic chamber (Perkin Elmer, Waltham, MA, USA) under anaerobic conditions (85% N₂, 10% CO₂, 5% H₂). Sterile discs were kept on these inoculated plates with the help of sterile forceps. Ag-CS-AA NC (10 µL) solution was placed on these discs and incubated at 37°C for 24 hrs in a bacterial incubator. Interpretation of the results was performed according to the NCCLS²⁹ to determine if the strain is resistant or susceptible to the tested antibiotics. Ag-CS-AA NC was suspended in 1 mL of deionized water and subjected to sonication for getting homogenized suspension³⁰. The effect of Ag-CS-AA NC was compared with that of the Polymyxin (disc loaded with 130 unit) and Kanamycin (disc loaded with 30 µg) as positive reference standard drugs. The breakpoint for susceptibility was a zone of inhibition of >11 mm. All of the NCCLS breakpoints for interpreting antibiotic susceptibility were used.

Hydrogen peroxide scavenging (H_2O_2) assay: H_2O_2 solution (40 mM) is prepared in phosphate buffer (50 mM pH 7.4). The concentration of hydrogen peroxide is determined by absorption at 240 nm using a spectrophotometer³¹. Graded concentrations of the Ag-CS-AA NC (10-60 μ g mL⁻¹) in distilled water are added to H_2O_2 and absorbance at 240 nm is determined after 1 min against a blank solution containing phosphate buffer without H_2O_2 . The percentage of H_2O_2 scavenging is calculated as follows:

Scavenged
$$H_2O_2$$
 (%) = $\frac{A_1 - A_2}{A_1} \times 100$

where, A_1 is the absorbance of control and A_2 is the absorbance of the test.

Experimental animals: The experimental animals used in this study were male albino Wistar rats (*Rattus norvegicus*, weight, 150±10 g) obtained from the National Research Center (Dokki, Giza, Egypt). The Rats were maintained under a 12:12-hrs light: dark cycle at 22-25°C in a well-ventilated animal facility (Department of Zoology, Faculty of Science, Cairo University). Autoclaved water and a commercial diet (Laboratory Rodent Diet 5001, Lab Diet, St Louis, MO) were provided without restriction. The animals were grouped (six per cage) and housed in static polycarbonate plastic cages (height, 20 cm, floor space, 860 cm²).

Experimental procedures: Rats were subjected to either Cecal Ligation and Puncture (CLP) or sham operation using aseptic techniques, according to Liu et al.32 Eighteen rats were divided into two main groups, the sham-operated control (6 rats) and the CLP group (12 rats). Sodium pentobarbital (50 mg kg⁻¹ b.wt.) was used to anaesthetize rats. The rat surgical area was sterilized with Betadine followed by a midline laparotomy. The cecum was identified, exteriorized and ligated just to the ileocecal valve to avoid intestinal obstruction. After ligation, the cecum was punctured using an 18-gauge needle to create two pores and squeeze gently to release a small amount of faecal content. Afterwards, the cecum was returned to the peritoneal cavity and then the muscle and skin were sutured using sterile suture (Black Braided Silk sutures 3/0, England). After the surgery, the animals were injected with 1 mL of saline subcutaneous for fluid restoration. Meanwhile, the sham-control rats were exhibited in the same procedures of CLP but the cecum was neither ligated nor punctured.

After 24 hrs of surgery, the CLP group was further divided into two subgroups (6 rats/subgroup). Subgroup one was administered distilled water, while subgroup two was administered 0.25 mg kg⁻¹ b.wt., Ag-CS-AA NC³³ daily for 3 days. Animals were euthanized on the 4th day of treatment under deep anaesthesia with an overdose of sodium pentobarbital (100 mg kg⁻¹ b.wt.)³⁴ and exsanguinated. Blood was collected for serum biochemistry, while liver and kidney tissues were collected for histology and biochemical analysis.

Biochemical analysis: The serum Aspartate Aminotransferase (AST) and Alanine Aminotransferase (ALT) were measured according to the method of Reitman and Frankel, serum Alkaline Phosphatase (ALP), serum γ -glutamyltransferase (GGT), serum creatinine, serum urea and serum uric acid were determined according to the manufacturer's instructions using Bio-diagnostic kits (Giza, Egypt).

Malondialdehyde (MDA), glutathione reduced (GSH), Nitric Oxide (NO) and Catalase (CAT)were determined in the liver and kidney homogenate supernatants according to the manufacture's instructions using Bio-diagnostic kits (Giza, Egypt).

Histopathological examination: The liver and kidney tissues were removed immediately, washed and fixed in neutral buffered formalin (10%) for further processing by the ordinary routine work: Dehydration, clearing and embedding. The paraffin-embedded blocks of the liver and kidney tissues were cut by using microtome in 4 μm-thick tissue sections. Hematoxylin and eosin (H and E) were used to stain tissue slices. The tissue sections were assessed under light microscopy independently by two investigators in a blinded way. The severity of tissue injury was scored 0: Absent, 1: Few, 2: Mild, 3: Moderate, to 4: Severe for each parameter. The parameters are cell vacuolization, nuclear fragmentation and cell necrosis³⁵. The histopathology scores were expressed as the sum of the individual scores. Ten high-power fields per sample were scored and averaged to represent each animal.

Statistical analysis: All results were expressed as Means±Standard Deviation (SD) of six animals. For variances estimation between the groups, one-way analysis of variance (ANOVA) with the Duncan post hoc test was used to compare between-group means using SPSS (SPSS Inc., Chicago, IL, USA) software. Values of p<0.05 were considered statistically significant.

RESULTS AND DISCUSSION

UV-visible spectral analysis: The absorption spectrum of the dark brown AgNPs suspension represented in Fig. 1a showed a surface Plasmon absorption band with a peak of 425 nm, which indicates the formation of Nano-sized particles of silver.

X-Ray Diffraction (XRD): XRD carried out the analysis of the crystalline size and structure of the Ag-CS-AA NC was shown in Fig. 1b. The numbers of Bragg reflections with 2 values of 38.30°, 44.61°, 64.67° and 77.73° indicated that the AgNPs were spherical structured and crystalline, while chitosan showed Bragg reflection with 2 values of 20°³⁶.

Transmission Electron Microscopy (TEM) analysis: The TEM analyses of AgNPs showed that the nanoparticles have spherical shapes and the size is ranged between 8 and 10 nm, as shown in Fig. 1c.

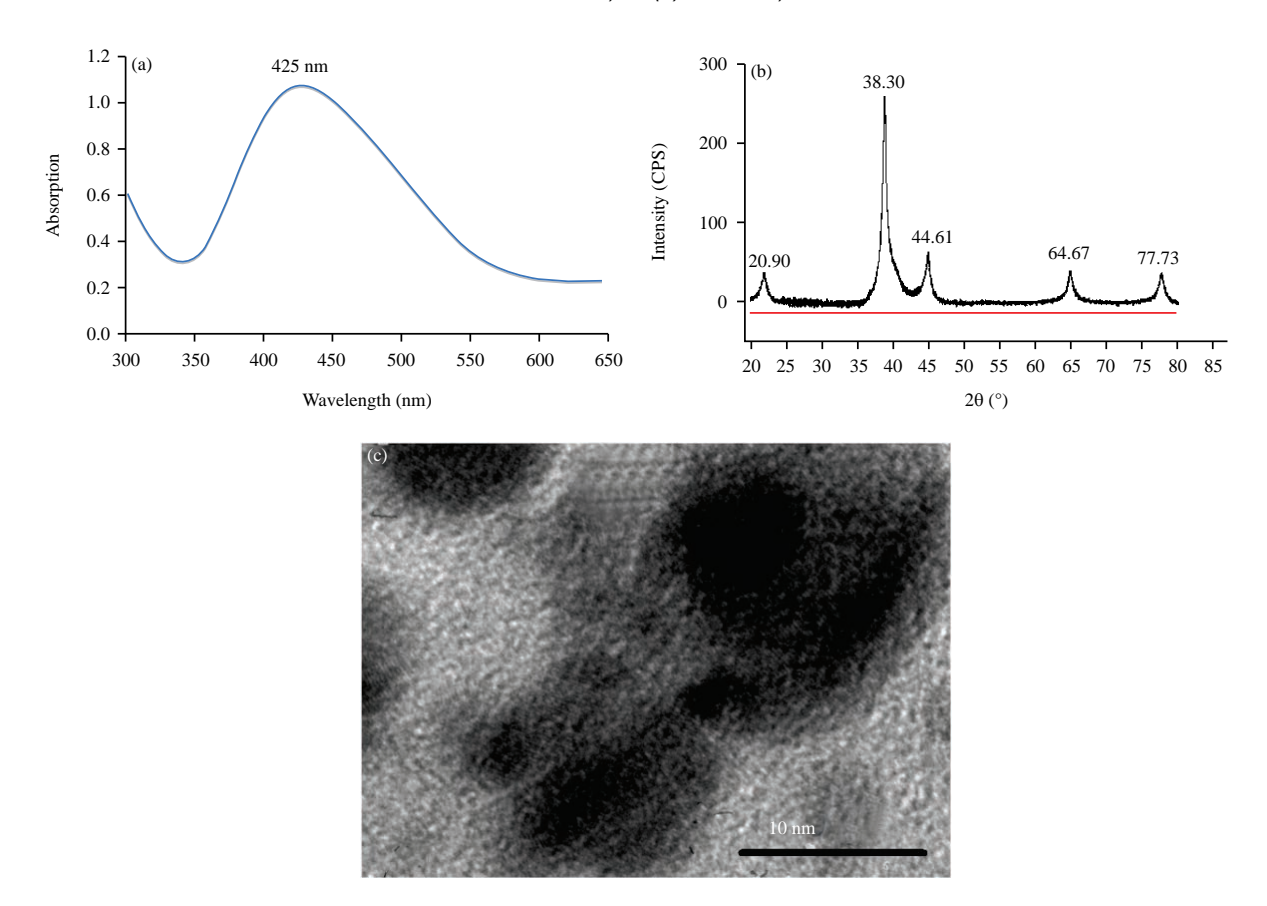


Fig. 1(a-c): Characterization of (a) AgNPs using UV-Visible spectral analysis, (b) XRD and (c) TEM analysis

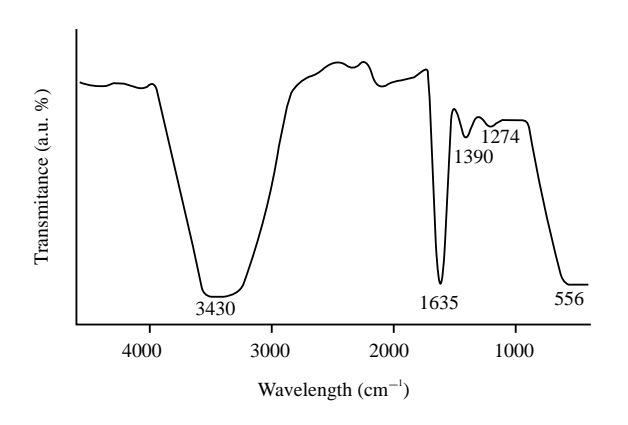


Fig. 2: FT-IR spectra of Ag-CS-AA NC

FTIR analysis: The FTIR spectrum of Ag NPs revealed absorption peaks at 3430, 1635, 1390, 1274 and 556 cm⁻¹, which correspond to amide linkage groups (Fig. 2). Moreover, the peaks around 3431 cm⁻¹ corresponded to OH group stretch vibrations. Because of the carbonyl stretch in proteins, the band at 1635 cm⁻¹ corresponded to amide I. The peak at 1390 cm⁻¹ denoted the symmetric deformation vibration mode of CH₃ and the one at 1274 cm⁻¹ corresponded to

the C-O stretching vibration of carboxylic acids. The peak at 556 cm⁻¹ belonged to the C-Br stretch of alkyl halides. The result identified the involvement of primary amino groups in the interaction with a metal surface and the amino groups were acted as capping sites for the Ag NPs stabilization³⁷.

XPS analysis: XPS analysis is used to examine the interaction of electron angular momentum with its spin and orbital angular momentum. The main elements of the Ag-CS-AA NC are carbon, oxygen, nitrogen and silver, which are presented in the wide spectrum. The spectrum was fitted by multiple Gaussians and normalized as indicated in Fig.3a-d. Upon ionization, Ag 3d region is characterized by two peaks due to their spin-orbital splitting that corresponds to Ag 3d_{5/2} and Ag $3d_{3/2}$ levels. For the metallic silver, the lines are observed at the Binding Energy (BE) of 368.2 and 374.2 eV. In the case of Ag-CS-AA NC, two lines appeared with lower BE as 366.6 and 372.2 eV, suggesting the presence of Agions (Fig. 3a). The C-C and C-H have peak was observed in C 1s spectrum at 285 eV (Fig. 3b). The bond AgO has a peak at 530.9 eV (Fig. 3c), while NH₂ groups have a peak at 397.8 eV (Fig. 3d), indicating that all nitrogen atoms are in the same vale. The nitrate ions

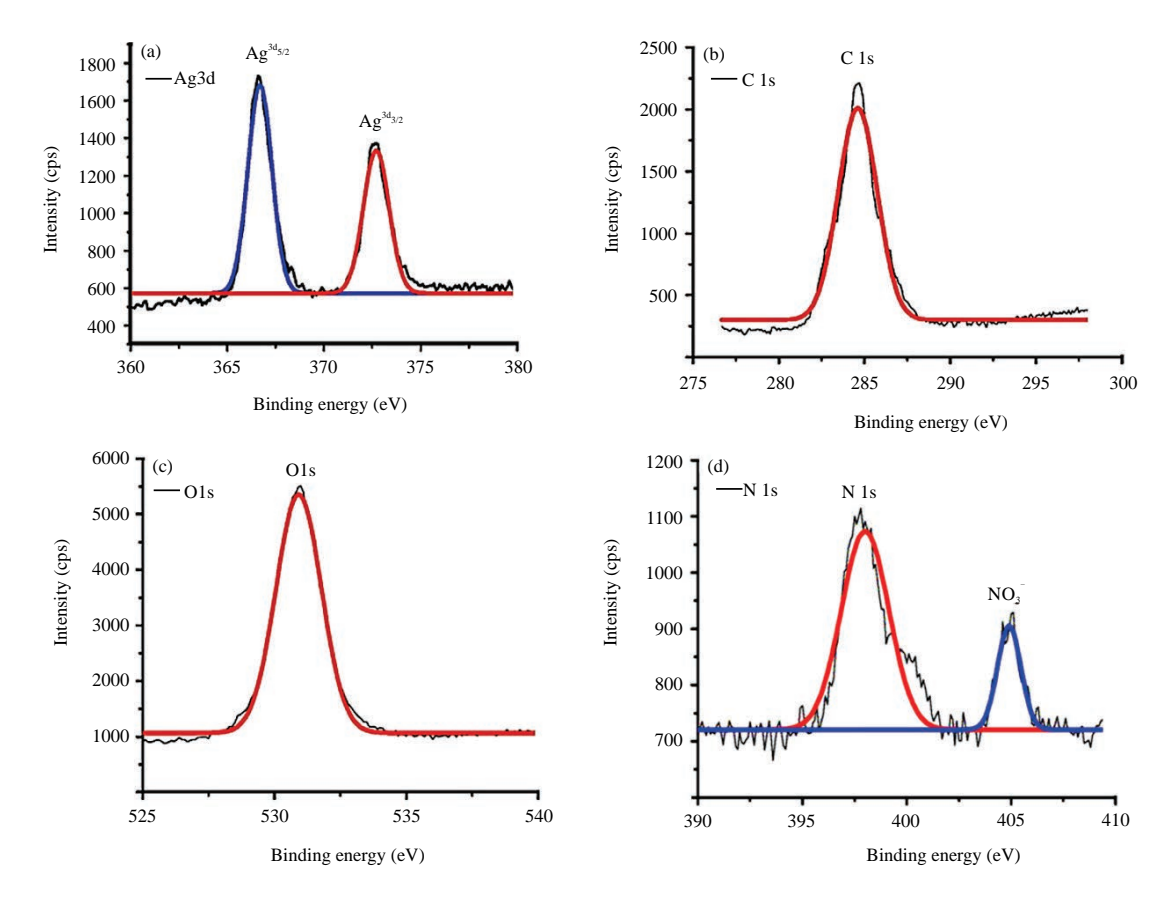


Fig. 3(a-d): XPS spectra of the biosynthesized Ag-CS-AA NC (a) Ag 3d, (b) C 1s spectra, (c) O 1s spectra and (d) N 1s spectra

Table 1: Effect of AgNPs on serum biochemical parameters of septic rats

					Bilirubin	Proteins	Albumin	Creatinine	Urea	Uric acid
Groups	AST (U L^{-1})	ALT (U L^{-1})	ALP (U L^{-1})	GGT (U L ⁻¹)	$(mg dL^{-1})$	$(g dL^{-1})$	$(g dL^{-1})$	$(mg dL^{-1})$	$(g dL^{-1})$	$(mg dL^{-1})$
Sham	150.37±5.52	114.88±8.55	94.05±4.43	17.52±1.93	0.71 ± 0.01	5.38±0.32	2.66±0.49	0.73±0.11	27.90±4.98	1.84±0.11
CLP	260.92 ± 6.04^{a}	188.73±6.33ª	165.43±8.83ª	43.73 ± 5.38^{a}	0.84 ± 0.08^a	6.66 ± 0.63^{a}	3.28 ± 0.38^a	1.32 ± 0.15^{a}	45.53±1.50°	2.36 ± 0.29^{a}
AgNPs	199.65±8.3°	157.89±7.86°	115.58±6.89°	19.51±2.76 ^b	0.71 ± 0.02^{b}	4.53±0.84 ^b	2.53±0.35 ^b	0.80 ± 0.13^{b}	38.09±3.12 ^b	2.00±0.25b

CLP: Cecal ligation and puncture, AUG: Augmentin, Values are Mean \pm SD (n = 6), a: Indicates statistical significance of compared to control group, b: Indicates statistical significance of compared to CLP groups

that remain from the silver nitrate precursor³⁸ are responsible for the additional peak at 405 eV (Fig. 3d). The interaction of Ag with the chitosan matrix may be the cause of Ag+ formation in the Ag-CS-AA NC. As a result of the XPS study, the Ag-CS-AA NC contains both Ag 3d and N 1s, confirming the presence of metal and chitosan in the Nanocomposite.

Ag-Measured concentration: The Nominal concentration for Ag-CS-AA NC was 8.45 mg Ag L^{-1} were corresponding to the measured concentration of AgNPs 0.25 mg Ag L^{-1} .

Antibacterial activity: Ag-CS-AA NC exhibits broad antibacterial activity against Gram-positive and Gram-negative

bacteria. The inhibition zone that appeared around the disc was measured and recorded as the antibacterial Ag-CS-AA NC, as shown in Fig. 4a.

 H_2O_2 scavenging activity: H_2O_2 scavenging activity represents the antioxidant activity of the substances. Ag-CS-AA NC showed H_2O_2 scavenging activity which increases with an increase in the concentrations (Fig. 4b).

Biochemical analysis: Enzyme activities of ALT, AST, ALP, GGT and concentrations of total proteins, albumin, creatinine, urea and uric acid of the CLP group showed a significant increase (p<0.05) as compared to the Sham group (Table 1).

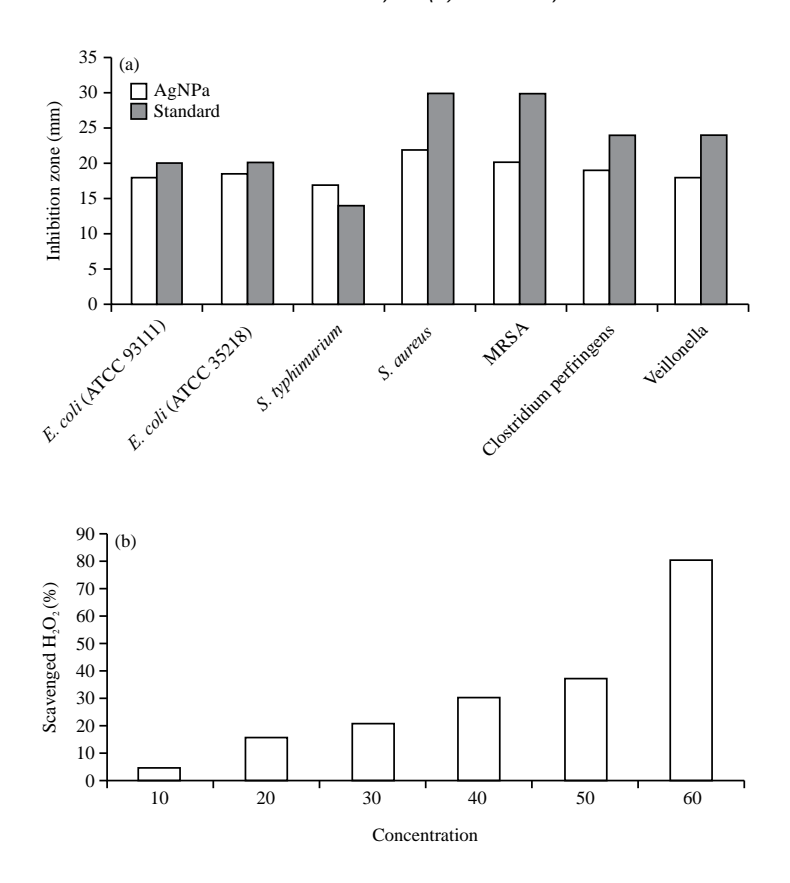


Fig. 4(a-b): Antibacterial activity of (a) Ag-CS-AA NC and (b) H₂O₂ scavenging activity

Table 2: Effect of AgNPs on liver oxidative stress parameters of septic rats

	MDA (nmol g^{-1} tissue)		NO (μmol L ⁻¹)		GSH (mg g ⁻¹ protein)		CAT (U g ⁻¹ protein)	
Groups	Liver	Kidney	Liver	Kidney	Liver	Kidney	Liver	Kidney
Sham	3.59±0.25	2.84±0.25	16.70±0.73	11.69±0.90	12.23±0.72	9.18±5.03	34.42±1.66	28.00±3.74
CLP	5.13±0.94ª	3.42 ± 0.14^{a}	21.86±0.81ª	15.18±0.91ª	8.29 ± 0.74^{a}	6.20 ± 2.99^a	26.89 ± 3.06^{a}	23.48±2.95ª
AgNPs	3.77±0.28 ^b	2.93±0.16 ^b	19.39±0.57°	13.27±0.26 ^b	10.47±2.16 ^b	8.81±4.75 ^b	31.26±2.20°	28.60±4.59 ^b

CLP: Cecal ligation and puncture, AUG: Augmentin, Values are Mean \pm SD (n=6), a: Indicates statistical significance of compared to control group, b: Indicates statistical significance of compared to CLP groups

While administration of Ag-CS-AA NC produced a significant decrease (p<0.05) in ALT, AST, ALP, GGT and concentrations of total proteins, albumin, creatinine, urea and uric acid compared with the CLP group.

Oxidative stress biomarkers: Liver and kidney MDA and NO concentrations were increased significantly (p<0.05) in the CLP group compared to the Sham group. However, significant decreases (p<0.05) in CAT activity and concentration of GSH were observed (Table 2). After three days of Ag-CS-AA NC treatment, there was a significant decrease (p<0.05) in the liver and kidney MDA and NO concentrations compared to the CLP group. Nevertheless, a significant increase (p<0.05) in CAT activity and concentration of GSH was noticed (Table 2).

Histopathological study: The liver section of Sham groups is formed of the classic hepatic lobules. Hepatocytes appeared polygonal in shape with rounded vesicular nuclei. Blood sinusoids were seen separating the cords of the liver cells and lined by flattened endothelial cells and Von Kupffer cells (Fig. 5a). Liver sections of septic rats revealed necrosis, apoptosis and loss of hepatic lobular (Fig. 5b). However, a liver section of septic rats treated with Ag-CS-AA NC showed improvement in the hepatic architecture and hepatic cells (Fig. 5c). Histologic liver injury scores of septic rats were significantly increased (p<0.05) compared to the Sham group. On the other hand, liver injury scores were significantly decreased (p<0.05) after the treatment with the Ag-CS-AA NC as compared to the CLP group (Fig. 5d).

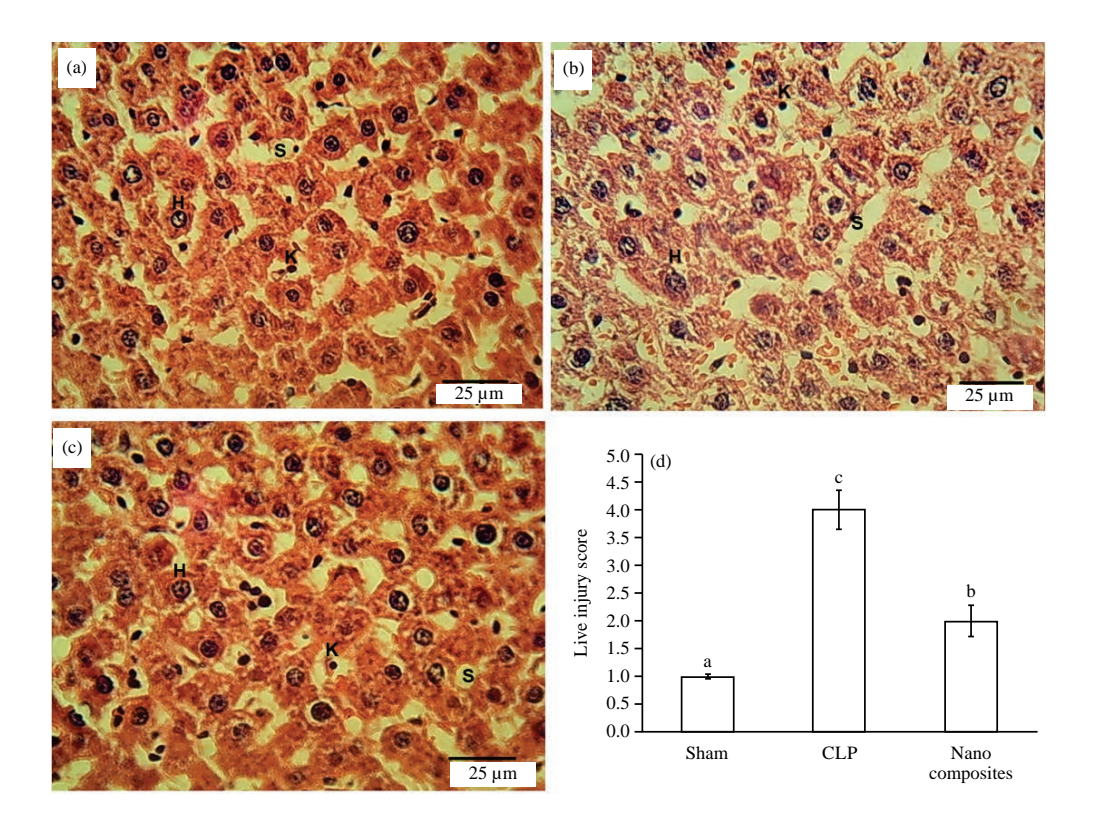


Fig. 5(a-d): Photomicrographs of liver sections

(a) Control group, (b) CLP group, (c) Ag-CS-AA NC treated group stained by hematoxylin and eosin (H and E) and (d) Represent the histologic liver injury scores of the 3 groups. Each value not sharing a common letter superscript is significantly different (p<0.05)

Histological investigation for a kidney is represented in Fig. 6a-d. Sham groups showed the typical architecture of the kidney with normal glomeruli (G) (Fig. 6a). Numerous alternations were observed in the kidney of septic rats include glomeruli endothelial cell proliferation, renal tubules epithelial cell degeneration and brush border loss (Fig. 6b). Besides, the score of kidney injury increased significantly (p<0.05) in the CLP group compared to the Sham group. After the treatment with Ag-CS-AA NC, an improvement in kidney histology of septic rats was noticed (Fig. 6c). Furthermore, a significant decrease (p<0.05) in a score of kidney injury was observed in the Ag-CS-AA NC treated group as compared to the CLP group (Fig. 6d).

Sepsis is recognized as a global public health problem caused by a dysregulated host response to infection³⁹. Using Nanocomposite as a new therapeutic strategy for sepsis treatment was described⁴⁰. The present study evaluated the therapeutic efficacy of chitosan-ascorbic acid-silver nanocomposites films against hepatorenal injury induced by CLP in rats. The present investigation used two essential NP formulation toxicity screening strategies to evaluate the safety and efficacy of the synthesized chitosan-ascorbic

acid-silver nanocomposites. The first one is the physicochemical characterization (size, surface area, shape, solubility). The second one is the elucidation of biological effects (*in vivo* studies)⁴¹.

Direct toxicity of newly synthesized compounds results from their chemical composition and surface reactivity⁴². Chitosan is usually used to synthesize metallic nanoparticles as it was a perfect example of a green and environmentally friendly synthesis^{27,18}. In the present study, chitosan serving as a reducing and stabilizing agent for silver nanoparticles (AgNPs), where AgNPs are bound to the chitosan-functional groups preventing NPs agglomeration²⁷. On the other hand, ascorbic acid was used as a reducing agent due to the presence of a large number of amino and hydroxyl groups, which decreased the time of reduction and growth thanks to many nucleation seeds²⁷. Thus, chitosan with ascorbic acid gave films with a uniform distribution of AgNPs.

The current study demonstrated the antibacterial activity of Ag-CS-AA NC against drug-resistant Gram-positive and Gram-negative bacteria. AgNPscan cause physical changes in the structure of the bacterial cell membrane, which leads to the destruction of these cells⁴³. Perhaps the silver link with the

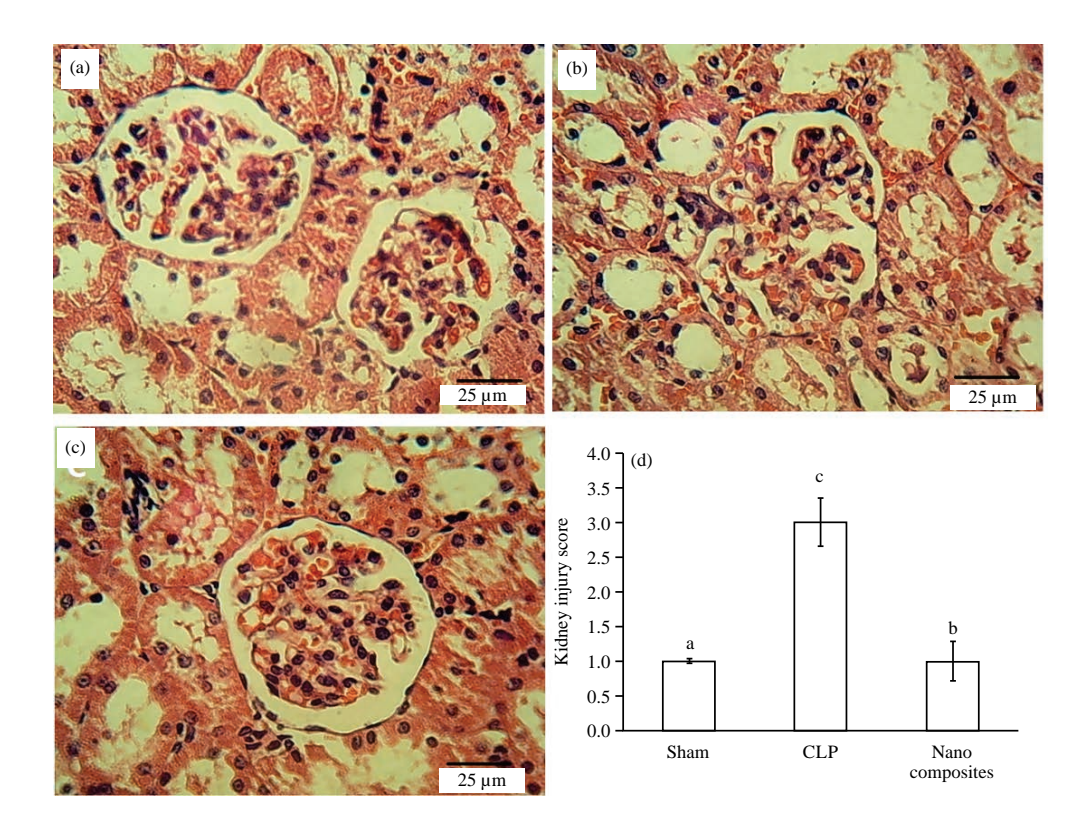


Fig. 6(a-d): Photomicrographs of kidney sections

(a) Control group, (b) CLP group, (c) Ag-CS-AA NC treated group stained by hematoxylin and eosin (H and E) and (d) Represent the histologic kidney injury scores of the 3 groups. Each value not sharing a common letter superscript is significantly different (p<0.05)

bacterial cells is due to the attraction between the positive charge of silver and the negative charge of the bacterial cell wall⁴⁴. Also, AgNPs ability to form free radicals is another way that silver uses to kill bacterial cells⁴⁵. Besides, chitosan itself is a well-known antibacterial⁴⁶. Chitosan's antibacterial ability is due to its binding to the outer cell protein A and destroying the cell wall⁴⁷. It is binding with bacteria mRNA, causing inhibition of protein synthesis⁴⁸.

It was observed that the effect of Ag-CS-AA NC during the current study on Gram-negative bacteria is higher than that of the Gram-positive, which could be due to the difference in the thickness of the bacterial cell wall as the thickness of the Gram-positive cells is much less than that of Gram-positive cells⁴⁹.

The induction of sepsis in rats by CLP is one of the most widely used models because it mimics sepsis in humans ⁵⁰. The liver is one of the most affected organs during infection, as it is involved in the disposal of infectious agents/products⁵¹. Hepatic impairment resulting from sepsis was confirmed in the current study by an increase in the levels of AST, ALT, ALP, GGT and bilirubin, with associated histological changes in the liver tissue. Systemic disturbances and inflammatory cytokines

and endotoxin effect are the leading causes of hepatic impairment during sepsis induction⁵².

The present study revealed that total proteins and albumin concentrations increased in septic rats comparing to Sham rats. Our results were in agreement with many previous studies 53,54 . The increase in total proteins in septic rats resulted from an increase in the synthesis of albumin and acute-phase proteins (such as $\alpha 1$ -acid glycoprotein, complement component C3 and transferrin) 55 . The septic rats also demonstrated increased protein synthetic capacity and increased translational efficiency, which is indicated by increased RNA activities 56 . Similarly, Vary and Kimball 54 indicated that the translation phase of protein synthesis in the liver increased 100 % in sepsis than Sham. The secretory hepatic protein syntheses after induction of sepsis play a role in host defence 57 .

On the other hand, the treatments with Ag-CS-AA NC restore the liver function parameter near normal level, which may be related to the potent antibacterial activates of these films. Additionally, ascorbic acid (vitamin C) is a powerful antioxidant that improves the antioxidant defence system of animals.

One of the most common organs affected during sepsis is the kidneys, resulting in sepsis associated-acute kidney injury that contributes to the morbidity and mortality of sepsis⁵⁸. Our results confirm that sepsis-induced kidney dysfunction increases serum creatinine, urea and uric acid concentration in the septic rat. The pathophysiological mechanisms of sepsis-associated acute kidney injury include renal hypotension and associated ischemia, tubular cell injury, inflammation and apoptosis⁵⁹. The hemodynamic fluctuations such as hypotension and reduced renal blood flow can induce renal ischemia and tissue hypoxia, leading to a decrease glomerular filtration rate⁶⁰. Besides, the oxidative stress leading to cell death may be the primary physiopathological process involved in sepsis-induced acute kidney injury⁶¹. The damage in the kidney of septic rats was confirmed by histopathological examination of kidney sections. On the other hand, the antibacterial activity of AgNPs and chitosan and antioxidant activity of ascorbic acid are the primary responses behind the improvement in the renal function parameters and histopathological section of the kidney in the treated septic rats.

Oxidative stress is one of the most important mechanisms associated with many diseases such as infection sepsis⁶². Oxidative stress results when the equilibrium between the internal antioxidant system and both Reactive Oxygen Species (ROS) and Reactive Nitrogen Species (RNS) is lost⁶³. The oxidative stress status of sepsis was confirmed in the current study by a significant increase in Malondialdehyde (MDA) and Nitric Oxide (NO) with a simultaneous decrease in the Glutathione reduced (GSH) and Catalase (CAT) activities in the tissues of the liver and kidney. During sepsis, ROS cause impairment of cells and organs by modulating the innate immune signalling cascade⁶⁴. Further damage due to oxidative condition results from NO's over-production, which known inhibitor of the mitochondrial electron transport chain⁶⁵.

The antioxidant activity of Ag-CS-AA NC may be due to the presence of ascorbic acid. Firstly, this suggestion was supported *in vitro* via the H_2O_2 scavenging activity of the Ag-CS-AA NC. Secondly, the antioxidant activity of the studies Ag-CS-AA NC was supported *in vivo* by decreasing MDA and NO concentrations and increasing GSH level and CAT activity in septic rats. Thus, inhibition of the bacterial activity and improvement of the antioxidant system is considered the main pathway for treating sepsis in rats using Ag-CS-AA NC.

CONCLUSION

Ag-CS-AA NC showed powerful antibacterial and antioxidant activities against sepsis in rats. The main

therapeutic pathways of these Nanocomposites include inhibition of bacterial growth using of AgNPs and chitosan and improve the antioxidant defence system of rats by ascorbic acid.

SIGNIFICANCE STATEMENT

This study discovers the antiseptics activities of Silver/chitosan/ascorbic acid Nanocomposites that can be beneficial for sepsis-induced by cecal ligation and puncture in rats. This study will help the researcher to uncover the critical area of septicemia that many researchers were not able to explore. Thus, a new theory on these Nano-materials combinations and possibly other combinations, may be arrived at.

ACKNOWLEDGMENT

This study was supported by the Researchers Supporting Project number (RSP-2021/25), King Saud University, Riyadh, Saudi Arabia.

REFERENCES

- Napolitano, L.M., 2018. Sepsis 2018: Definitions and guideline changes. Surg. Infect., 19: 117-125.
- Tavasoli, S., A.H. Zarnani, M. Vafa, M. Moradi-Lakeh, H. Pazoki-Toroudi and S. Eghtesadi, 2014. The effect of pomegranate extract on survival and peritoneal bacterial load in cecal ligation and perforation model of sepsis in rats. Int. J. Prev. Med., 5: 104-109.
- 3. Minasyan, H., 2019. Sepsis: Mechanisms of bacterial injury to the patient. Scand. J. Trauma, Resuscitation Emergency Med., Vol. 27. 10.1186/s13049-019-0596-4.
- Dolin, H.H., T.J. Papadimos, X. Chen and Z.K. Pan, 2019. Characterization of pathogenic sepsis etiologies and patient profiles: A novel approach to triage and treatment. Microbiol. Insights, Vol. 12. 10.1177/1178636118825081.
- Fleischmann, C., A. Scherag, N.K.J. Adhikari, C.S. Hartog and T. Tsaganos *et al.*, 2016. Assessment of global incidence and mortality of hospital-treated sepsis. current estimates and limitations. Am. J. Respir. Crit. Care Med., 193: 259-272.
- Ono, S., H. Tsujimoto, S. Hiraki and S. Aosasa, 2018. Mechanisms of sepsis-induced immunosuppression and immunological modification therapies for sepsis. Ann. Gastroenterological Surg., 2: 351-358.
- 7. Eidt, M.V., F.B. Nunes, L. Pedrazza, G. Caeran and G. Pellegrin *et al.*, 2016. Biochemical and inflammatory aspects in patients with severe sepsis and septic shock: The predictive role of IL-18 in mortality. Clin. Chim. Acta, 453: 100-106.

- Sadek, S.A., S.S. Hassanein, A.S. Mohamed, A.M. Soliman and S.R. Fahmy, 2021. Echinochrome pigment extracted from sea urchin suppress the bacterial activity, inflammation, nociception and oxidative stress resulted in the inhibition of renal injury in septic rats. J. Food Biochem., Vol. 2021. 10.1111/jfbc.13729.
- Campos, M., R. Capilla, F. Naya, R. Futami and T. Coque et al., 2019. Simulating multilevel dynamics of antimicrobial resistance in a membrane computing model. mBio, Vol. 10. 10.1128/mbio.02460-18.
- Salem, S.S. and A. Fouda, 2021. Green synthesis of metallic nanoparticles and their prospective biotechnological applications: An overview. Biol. Trace Elem. Res., 199: 344-370.
- 11. Hashem, A.H., A.M.A. Khalil, A.M. Reyad and S.S. Salem, 2021. Biomedical applications of mycosynthesized selenium nanoparticles using *Penicillium expansum* ATTC 36200. Biol. Trace Elem. Res., 10.1007/s12011-020-02506-z.
- Mamdouh, S., A.S. Mohamed, H.A. Mohamed and W.S. Fahmy, 2021. The effect of zinc concentration on physiological, immunological and histological changes in crayfish (*Procambarus clarkii*) as bio-indicator for environment quality criteria. Biol. Trace Elem. Res., Vol. 2021. 10.1007/s12011-021-02653-x.
- Abu-Elghait, M., M. Hasanin, A.H. Hashem and S.S. Salem, 2021. Ecofriendly novel synthesis of tertiary composite based on cellulose and myco-synthesized selenium nanoparticles: Characterization, antibiofilm and biocompatibility. Int. J. Biol. Macromol., 175: 294-303.
- Rai, M.K., S.D. Deshmukh, A.P. Ingle and A.K. Gade, 2012.
 Silver nanoparticles: The powerful nanoweapon against multidrug-resistant bacteria. J. Appl. Microbiol., 112:841-852.
- 15. Sim, W., R.T. Barnard, M.A.T. Blaskovich and Z.M. Ziora, 2018. Antimicrobial silver in medicinal and consumer applications: A patent review of the past decade (2007–2017). Antibiotics, Vol. 7. 10.3390/antibiotics7040093.
- 16. Soliman, H., A. Elsayed and A. Dyaa, 2018. Antimicrobial activity of silver nanoparticles biosynthesised by *Rhodotorula* sp. strain ATL72. Egypt. J. Basic Applied Sci., 5: 228-233.
- 17. Sondi, I. and B. Salopek-Sondi, 2004. Silver nanoparticles as antimicrobial agent: A case study on *E. coli* as a model for Gram-negative bacteria. J. Colloid Interface Sci., 275: 177-182.
- Kalaivani, R., M. Maruthupandy, T. Muneeswaran, A.H. Beevi, M. Anand, C.M. Ramakritinan and A.K. Kumaraguru, 2018. Synthesis of chitosan mediated silver nanoparticles (Ag NPs) for potential antimicrobial applications. Front. Lab. Med., 2: 30-35.
- Alsharif, S.M., S.S. Salem, M.A. Abdel-Rahman, A. Fouda and A.M. Eid *et al.*, 2020. Multifunctional properties of spherical silver nanoparticles fabricated by different microbial taxa. Heliyon, Vol. 6. 10.1016/j.heliyon.2020.e03943.

- Salem, S.S., E.F. EL-Belely, G. Niedbała, M.M. Alnoman and S.E.D. Hassan *et al.*, 2020. Bactericidal and *in-vitro* cytotoxic efficacy of silver nanoparticles (Ag-NPs) fabricated by endophytic actinomycetes and their use as coating for the textile fabrics. Nanomaterials, Vol. 10. 10.3390/nano10 102082.
- 21. Aref, M.S. and S.S. Salem, 2020. Bio-callus synthesis of silver nanoparticles, characterization and antibacterial activities via *Cinnamomum camphora* callus culture. Biocatal. Agric. Biotechnol., Vol. 27. 10.1016/j.bcab.2020.101689.
- Eid, A.M., A. Fouda, G. Niedbała, S.E.D. Hassan and S.S. Salem *et al.*, 2020. Endophytic *Streptomyces laurentii* mediated green synthesis of Ag-NPs with antibacterial and anticancer properties for developing functional textile fabric properties. Antibiotics, Vol. 9. 10.3390/antibiotics9100641.
- Mohamed, A.S., S.B. Dajem, M. Al-Kahtani, S.B. Ali, E. Ibrahim, K. Morsy and S.R. Fahmy, 2021. Silver/chitosan nanocomposites induce physiological and histological changes in freshwater bivalve. J. Trace Elem. Med. Biol., Vol. 65. 10.1016/j.jtemb.2021.126719.
- 24. Joshi, J.M. and V.K. Sinha, 2007. Ceric ammonium nitrate induced grafting of polyacrylamide onto carboxymethyl chitosan. Carbohydr. Polym., 67: 427-435.
- 25. Raafat, D. and H.G. Sahl, 2009. Chitosan and its antimicrobial potential-a critical literature survey. Microb. Biotechnol., 2: 186-201.
- Pakseresht, S., A.W.M. Alogaili, H. Akbulut, D. Placha and E. Pazdziora et al., 2019. Silver/chitosan antimicrobial nanocomposites coating for medical devices: Comparison of nanofiller effect prepared via chemical reduction and biosynthesis. J. Nanosci. Nanotechnol., 19: 2938-2942.
- Regiel-Futyra, A., M. Kus-Liśkiewicz, V. Sebastian, S. Irusta, M. Arruebo, A. Kyzioł and G. Stochel, 2017. Development of noncytotoxic silver-chitosan nanocomposites for efficient control of biofilm forming microbes. RSC Adv., 7: 52398-52413.
- Dananjaya, S.H.S., D.C.M. Kulatunga, G.I. Godahewa, C. Nikapitiya and C. Oh *et al.*, 2017. Preparation, characterization and antimicrobial properties of chitosansilver nanocomposites films against fish pathogenic bacteria and fungi. Indian J. Microbiol., 57: 427-437.
- 29. Balouiri, M., M. Sadiki and S.K. Ibnsouda, 2016. Methods for *in vitro* evaluating antimicrobial activity: A review. J. Pharm. Anal., 6: 71-79.
- 30. Morones, J.R., J.L. Elechiguerra, A. Camacho, K. Holt, J.B. Kouri, J.T. Ramirez and M.J. Yacaman, 2005. The bactericidal effect of silver nanoparticles. Nanotechnology, 16: 2346-2353.
- 31. Fernando, C.D. and P. Soysa, 2015. Optimized enzymatic colorimetric assay for determination of hydrogen peroxide (H_2O_2) scavenging activity of plant extracts. MethodsX, 2: 283-291.

- 32. Liu, M.W., M.X. Su, W. Zhang, Y.H. Wang and L.F. Qin *et al.*, 2015. Effect of *Melilotus suaveolens* extract on pulmonary microvascular permeability by downregulating vascular endothelial growth factor expression in rats with sepsis. Mol. Med. Rep., 11: 3308-3316.
- 33. Elbehiry, A., M. Al Dubaib, E. Marzouk and I. Moussa, 2018. Antibacterial effects and resistance induction of silver and gold nanoparticles against *Staphylococcus aureus* induced mastitis and the potential toxicity in rats. Microbiol. Open, Vol. 8. 10.1002/mbo3.698.
- 34. Mohamed, A.S., M. Hosney, H. Bassiony, S.S. Hassanein, A.M. Soliman, S.R. Fahmy and K. Gaafar, 2020. Sodium pentobarbital dosages for exsanguination affect biochemical, molecular and histological measurements in rats. Sci. Rep., Vol. 10. 10.1038/s41598-019-57252-7.
- 35. Yang, J., R. Wu, X. Qiang, M. Zhou and W. Dong *et al.*, 2009. Human adrenomedullin and its binding protein attenuate organ injury and reduce mortality after hepatic ischemia-reperfusion. Ann. Surg., 249: 310-317.
- 36. Ali, S.W., S. Rajendran and M. Joshi, 2011. Synthesis and characterization of chitosan and silver loaded chitosan nanoparticles for bioactive polyester. Carbohydr. Polym., 83: 438-446.
- Potara, M., M. Baia, C. Farcau and S. Astilean, 2012. Chitosan-coated anisotropic silver nanoparticles as a SERS substrate for single-molecule detection. Nanotechnology, Vol. 23. 10.1088/0957-4484/23/5/055501.
- 38. Prokhorov, E., S. Kumar-Krishnan, G. Luna-Barcenas, M.V. Lepe and B. Campos, 2015. Structure and properties of chitosansilver nanoparticles nanocomposites. Curr. Nanosci., 11: 166-174.
- 39. Markwart, R., H. Saito, T. Harder, S. Tomczyk and A. Cassini *et al.*, 2020. Epidemiology and burden of sepsis acquired in hospitals and intensive care units: A systematic review and meta-analysis. Intensive Care Med., 46: 1536-1551.
- 40. Pant, A., I. Mackraj and T. Govender, 2021. Advances in sepsis diagnosis and management: A paradigm shift towards nanotechnology. J. Biomed. Sci., Vol. 28. 10.1186/s12929-020-00702-6
- 41. Oberdorster, G., A. Maynard, K. Donaldson, V. Castranova and J. Fitzpatrick *et al.*, 2005. Principles for characterizing the potential human health effects from exposure to nanomaterials: Elements of a screening strategy. Particle Fibre Toxicol., Vol. 2. 10.1186/1743-8977-2-8.
- 42. Navarro, E., A. Baun, R. Behra, N.B. Hartmann and J. Filser *et al.*, 2008. Environmental behavior and ecotoxicity of engineered nanoparticles to algae, plants and fungi. Ecotoxicology, 17: 372-386.
- 43. Seong, M. and D.G. Lee, 2017. Silver nanoparticles against *Salmonella* enterica serotype typhimurium: Role of inner membrane dysfunction. Curr. Microbiol., 74: 661-670.

- 44. Abbaszadegan, A., Y. Ghahramani, A. Gholami, B. Hemmateenejad, S. Dorostkar, M. Nabavizadeh and H. Sharghi, 2015. The effect of charge at the surface of silver nanoparticles on antimicrobial activity against gram-positive and gram-negative bacteria: A preliminary study. J. Nanomater., Vol. 2015. 10.1155/2015/720654.
- 45. Prabhu, S. and E.K. Poulose, 2012. Silver nanoparticles: Mechanism of antimicrobial action, synthesis, medical applications and toxicity effects. Int. Nano Lett., Vol. 2. 10.1186/2228-5326-2-32.
- 46. Ll, B., C.L. Shan, M.Y. Ge, L. Wang and Y. Fang, 2013. Antibacterial mechanism of chitosan and its applications in protection of plant from bacterial disease. Asian J. Chem., 25: 10033-10036.
- 47. Goy, R.C., S.T.B. Morais and O.B.G. Assis, 2016. Evaluation of the antimicrobial activity of chitosan and its quaternized derivative on *E. coli* and *S. aureus* growth. Rev. Bras. Farmacognosia, 26: 122-127.
- 48. Archana, D., B.K. Singh, J. Dutta and P.K. Dutta, 2015. Chitosan-PVP-nano silver oxide wound dressing: *in vitro* and *in vivo* evaluation. Int. J. Biol. Macromol., 73: 49-57.
- Chatterjee, T., B.K. Chatterjee, D. Majumdar and P. Chakrabarti, 2015. Antibacterial effect of silver nanoparticles and the modeling of bacterial growth kinetics using a modified Gompertz model. Biochim. Biophys. Acta (BBA) Gen. Subjects, 1850: 299-306.
- 50. Hubbard, W.J., M. Choudhry, M.G. Schwacha, J.D. Kerby, L.W. Rue, K.I. Bland and I.H. Chaudry, 2005. Cecal ligation and puncture. Shock, 24: 52-57.
- 51. Nesseler, N., Y. Launey, C. Aninat, F. Morel, Y. Mallédant and P. Seguin, 2012. Clinical review: The liver in sepsis. Crit. Care, Vol. 16. 10.1186/cc11381.
- 52. Wang, D., Y. Yin and Y. Yao, 2014. Advances in sepsis-associated liver dysfunction. Burns Trauma, Vol. 2. 10.4103/23 21-3868.132689.
- 53. Mohamed, A.S., S.A. Sadek, S.S. Hassanein and A.M. Soliman, 2019. Hepatoprotective effect of echinochrome pigment in septic rats. J. Surg. Res., 234: 317-324.
- Ruot, B., I. Papet, F. Béchereau, P. Denis and C. Buffière et al.,
 2003. Increased albumin plasma efflux contributes to hypoalbuminemia only during early phase of sepsis in rats.
 Am. J. Physiol. Regul. Integr. Comp. Physiol., 284: R707-R713.
- 55. Cray, C., 2012. Acute phase proteins in animals. Prog. Mol. Biol. Transl. Sci., 105: 113-150.
- O'Leary, M.J., C.N. Ferguson, M.J. Rennie, C.J. Hinds, J.H. Coakley and V.R. Preedy, 2001. Sequential changes in in vivo muscle and liver protein synthesis and plasma and tissue glutamine levels in sepsis in the rat. Clin. Sci. (Lond)., 101: 295-304.
- 57. Strnad, P., F. Tacke, A. Koch and C. Trautwein, 2016. Liver-guardian, modifier and target of sepsis. Nat. Rev. Gastroenterol. Hepatol., 14: 55-66.

- 58. Poston, J.T. and J.L. Koyner, 2019. Sepsis associated acute kidney injury. BMJ, Vol. 364. 10.1136/bmj.k4891.
- 59. Maiden, M.J., S. Otto, J.K. Brealey, M.E. Finnis and M.J. Chapman *et al.*, 2016. Structure and function of the kidney in septic shock. A prospective controlled experimental study. Am. J. Respir. Crit. Care Med., 194: 692-700.
- 60. Bellomo, R., J.A. Kellum, C. Ronco, R. Wald and J. Martensson *et al.*, 2017. Acute kidney injury in sepsis. Intensive Care Med., 43: 816-828.
- 61. Vasco, C.F., M. Watanabe, C. Fonseca and M.F. Vattimo, 2018. Sepsis-induced acute kidney injury: Kidney protection effects by antioxidants. Rev. Bras. Enferm., 71: 1921-1927.
- 62. Sakaguchi, S. and S. Furusawa, 2006. Oxidative stress and septic shock: Metabolic aspects of oxygen-derived free radicals generated in the liver during endotoxemia. FEMS Immunol. Med. Microbiol., 47: 167-177.
- 63. Bar-Or, D., M.M. Carrick, C.W. Mains, L.T. Rael, D. Slone and E.N. Brody, 2015. Sepsis, oxidative stress and hypoxia: Are there clues to better treatment? Redox Rep., 20: 193-197.
- 64. Barichello, T., J.J. Fortunato, Â.M. Vitali, G. Feier and A. Reinke *et al.*, 2006. Oxidative variables in the rat brain after sepsis induced by cecal ligation and perforation. Crit. Care Med., 34: 886-889.
- 65. Brealey, D. and M. Singer, 2003. Mitochondrial dysfunction in sepsis. Curr. Infect. Dis. Rep., 5: 365-371.